Influence of Water on Tribolayer Growth When Lubricating Steel with a Fluorinated Phosphonium Dicyanamide Ionic Liquid

Luigi A. Urtis[1,2], Andrea Arcifa[2], Peng Zhang [3§], Junxiao Du[2], Marzia Fantauzzi[1], Daniel Rauber[4], Rolf Hempelmann[4], Tobias Kraus[3,5], Antonella Rossi[1,2], Nicholas D. Spencer[2]

[1]Department of Chemical and Geological Sciences, University of Cagliari, Campus of Monserrato (CA), I09042 Monserrato

[2]Laboratory for Surface Science and Technology, Department of Materials, ETH Zurich, HCI H 523, Vladimir-Prelog-Weg 5, CH-8093 Zürich, Switzerland

[3]INM - Leibniz Institute for New Materials, Campus D2 2, 66123 Saarbrücken, Germany

[4] Transfer center Sustainable Electrochemistry, Saarland University and KIST Europe, Am Markt, Zeile 3, 66125 Saarbrücken, Germany.

[5] Colloid and Interface Chemistry, Saarland University, Campus D2 2, 66123 Saarbrücken, Germany

[§]Current address: School of Materials Science and Engineering, Key Laboratory for Polymeric Composite and Functional Materials of Ministry of Education, Sun Yat-sen University, Guangzhou 510275, China

Supplementary Information

S 1. Tribological testing at different loads in a nitrogen atmosphere

The optical micrographs of the tests carried out in the presence of a nitrogen atmosphere, applying three different loads with a constant sliding velocity (1.25 mm/s) at room temperature are shown in Figure S1.

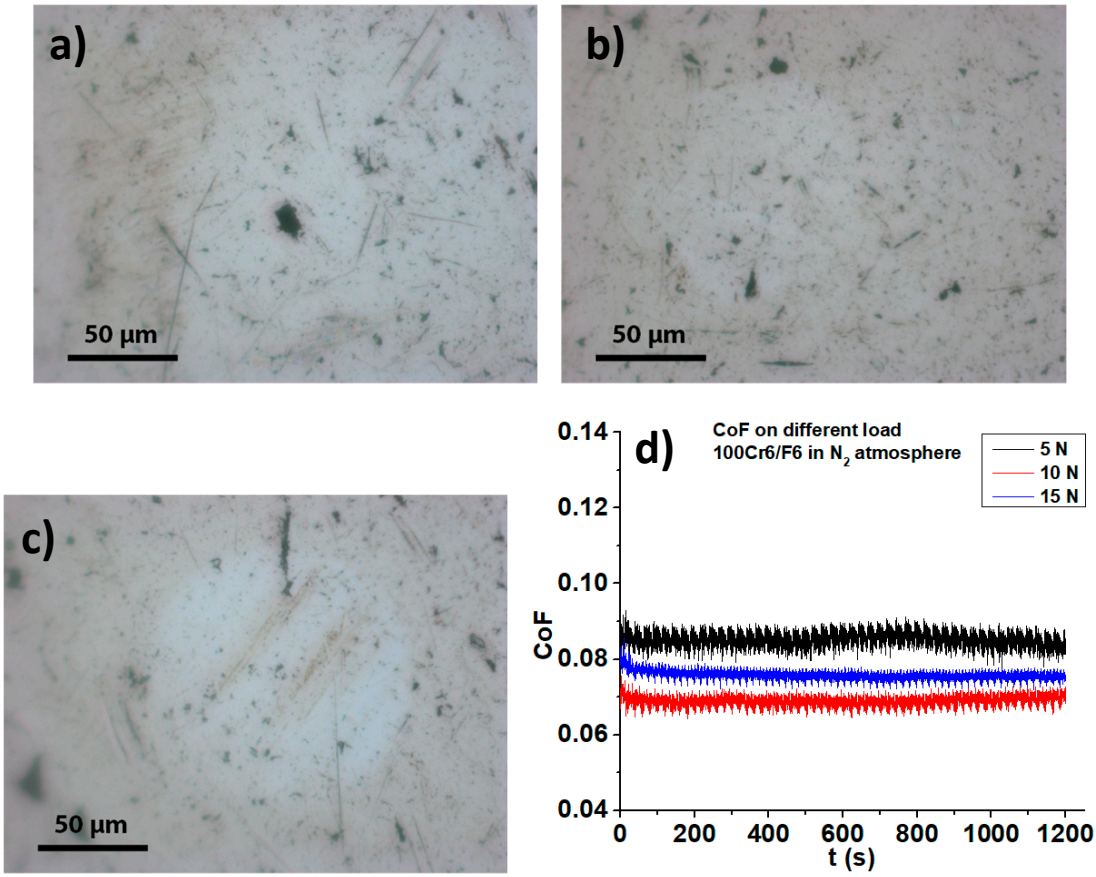

Figure S1. Optical images of 100Cr6 ball after pin-on-disk tribotests using the IL F6 as lubricant applying different load: **a**) 5 N, **b**) 10 N, and **c**) 15 N. All the tests were carried out with a constant sliding speed of 1.25 mm/s and a duration of 20 min in nitrogen atmosphere and room temperature (21 ± 1 °C). **d**) Frictional traces for the pin-on-disk tribotests using the IL F6 as lubricant applying different load – 5 N (black), 10 N (red), 15 N (blue). All tests were carried out with a constant sliding speed of 1.25 mm/s and a duration of 20 min in nitrogen atmosphere and room temperature (21 ± 1 °C).

S 2. Tribotests in humid air

Figure S2 shows the optical micrographs of the steel disk track for the pin-on-disk tribotest carried out in the presence of the ionic liquid F6 as lubricant at a constant sliding speeds of 1.25 mm/s and applying a constant load of 5 N for 20 min. The test was run in the presence of humid air (35 ± 5 °C) at room temperature (21 ± 1 °C).

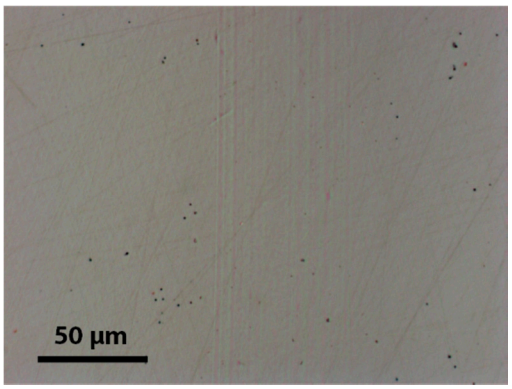

Figure S2. Optical image of 100Cr6 disk after pin-on-disk tribotest using the IL F6 as lubricant at 35 ± 5 % RH and 21 ± 1 °C. The test was carried out with an applied load of 5 N and a duration of 20 min at room temperature. Constant sliding speed: 1.25 mm/s.

S 3. Small area XPS analysis on 100Cr6 pin tribostressed in humid air

The chemical composition of the deposit formed over the contact area of the pin tested in the presence of humid air (Figure 2a) was obtained by X-ray photoelectron spectroscopy. The curve-fitting parameters for the spectra acquired on both the contact and non-contact area are listed in Table S1.

Table S1a. Curve-fitting parameters of the most intense photoelectron lines of the elements detected in the noncontact area (NC) of the pin after tribo-testing. The binding energies, FWHM of the peak heights and line shapes are provided together with the proposed assignment of the components.

Signal	BE (eV)	FWHM (eV)	Line shape	Assignment
Fe 2p	706.8 ± 0.1	1.0	GL(85)T(0.63)	Fe(0)
	709.3 ± 0.1	2.1	GL(40)	Fe(II)
	714.8 ± 0.1	2.1	GL(40)	Fe(II) sat.
	710.7 ± 0.1	2.1	GL(45)	Fe(III)
	712.2 ± 0.1	2.9	GL(45)	Fe(III) ox-hy
	713.6 ± 0.1	1.5	GL(60)T(1)	Fe (III) phosphate
C 1s	283.2 ± 0.1	1.3	GL(30)	Carbide
	285.0 ± 0.1	1.3	GL(30)	Aliphatic C
	286.3 ± 0.1	1.3	GL(30)	C-O, C-P
	287.8 ± 0.1	1.3	GL(30)	C=O
	288.8 ± 0.1	1.3	GL(30)	COOX, carbonates
	290.2 ± 0.1	1.3	GL(30)	C-F
O 1s	530.1 ± 0.1	1.3	GL(30)	Fe oxides
	531.6 ± 0.1	1.3	GL(30)	O metal hydroxide, Phosphate
	532.6 ± 0.1	1.3	GL(30)	COOX, carbonates
	533.8 ± 0.1	1.5	GL(30)	Adsorbed H_2O

P 2p	133.1 ± 0.1	1.7	GL(30)	Phosphate (Ca, Fe)
F 1s	684.7 ± 0.1	1.7	GL(40)	CaF_2
	688.7 ± 0.1	1.7	GL(40)	C-F
Ca 2p	347.6 ± 0.1	1.5	GL(50)	$CaCO_3$, $Ca_3(PO_4)_2$

Table S1b. Curve-fitting parameters of the most intense photoelectron lines of the elements detected on the contact area (C) of the pin after the tribo-test. The binding energies, FWHM of the peak heights and line shapes are provided together with the proposed assignment of the components.

Signal	**BE (eV)**	**FWHM (eV)**	**Line shape**	**Assignment**
Fe 2p	706.7 ± 0.1	1.0	GL(85)T(0.63)	Fe(0)
	709.3 ± 0.1	2.1	GL(40)	Fe(II)
	714.8 ± 0.1	2.1	GL(40)	Fe(II) sat.
	710.7 ± 0.1	2.1	GL(45)	Fe(III)
	712.1 ± 0.1	2.9	GL(45)	Fe(III) ox-hy
	713.7 ± 0.1	1.5	GL(60)T(1)	Fe(III) phosphate
C 1s	283.0 ± 0.1	1.3	GL(30)	Carbide
	285.0 ± 0.1	1.3	GL(30)	Aliphatic C
	286.5 ± 0.1	1.3	GL(30)	C-O, C-P, C-N
	288.2 ± 0.1	1.3	GL(30)	C=O
	289.3 ± 0.1	1.3	GL(30)	COOX, carbonates, C(O)N
	293.1 ± 0.1	1.3	GL(30)	C-F
O 1s	530.0 ± 0.1	1.3	GL(30)	Fe oxides
	531.6 ± 0.1	1.3	GL(30)	O metal hydroxide, Phosphate
	532.7 ± 0.1	1.3	GL(30)	COOX, carbonates, C(O)N
P 2p	133.2 ± 0.1	1.7	GL(30)	Phosphate (Ca, Fe)
F 1s	684.8 ± 0.1	1.7	GL(40)	CaF_2

	687.1 ± 0.1	1.7	GL(40)	C-F
Ca 2p	348.0 ± 0.1	1.5	GL(50)	$CaCO_3$, $Ca_3(PO_4)_2$, CaF_2
N 1s	399.2 ± 0.1	1.4	GL(45)	N-C
	400.2 ± 0.1	1.4	GL(45)	C(O)N
	401.8 ± 0.1	1.4	GL(45)	R_4N^+

The *apparent concentrations* of the chemical species are measured by correcting the intensities of the signal by relative sensitivity factors using the *first principle method*[1,2]. The results, for contact and non-contact area, are reported in Table S2.

It has to be emphasized that this approach should be only used when the sample is homogenous over the depth probed by the technique. This is clearly not the case for the heterogeneous tribofilms investigated in this work that are very complex being patchy and not homogeneous in depth. On the other hand, semi-quantitative information might be obtained when comparing the apparent concentrations of the species that are present on this kind of sample surface.

Table S2. Apparent concentration of detected species (at%) of the no-contact area and the contact area for the pin tribostressed using the IL F6 as lubricant obtained by small area XPS. Pin-on-disk test conditions: sliding speed 1.25 mm/s; load 5 N; RH: 35 ± 5; T: 21 ± 1 °C; t: 20 min.

Element	**Component/Assignment**	**No-Contact (NC)**	**Contact (C)**
Fe 2p*	Fe(II)	3.2 at%	1.7 at%
	Fe(III)	4.7 at%	3.0 at%
	Fe(III) ox-hy	3.6 at%	2.6 at%
	Fe(III) phosphate	-	0.3 at%
C 1s*	Aliphatic C	28.6 at%	25.5 at%
	C-O	3.9 at%	3.5 at%

	C=O	1.7 at%	2.6 at%
	COOX, carbonates, C(O)N	3.5 at%	1.5 at%
	C-F	0.5 at%	0.3 at%
O 1s	Fe oxides	27.7 at%	16.1 at%
	O metal hydroxide, Phosphate	13.2 at%	12.5 at%
	COOX, carbonates, C(O)N	4.7 at%	5.0 at%
	H_2O	0.8 at%	-
P 2p	Phosphate (Ca, Fe)	2.4 at%	2.3 at%
F 1s	CaF_2	0.2 at%	12.5 at%
	C-F	0.4 at%	0.7 at%
Ca 2p	$CaCO_3$, $Ca_3(PO_4)_2$, CaF_2	0.8 at%	8.6 at%
N 1s	N-C	-	0.5 at%
	C(O)N	-	0.5 at%
	R_4N^+	-	0.2 at%

***** The components ascribed to Fe(0) and carbide were not take into account for the surface tribolayer because they belong to the alloy bulk.

S 4. NMR, ESI-MS, XPS and ATR FT-IR characterization of the ionic liquid

The ionic liquid was characterized by ATR FT-IR spectroscopy, nuclear magnetic resonance (NMR), electrospray ionization mass spectrometry (ESI-MS) and X-ray photoelectron spectroscopy (XPS)

In the following the ^{1}H NMR, $^{13}C\{^{1}H\}$ NMR, $^{19}F\{^{1}H\}$ NMR, $^{31}P\{^{1}H\}$ NMR are provided.
^{1}H NMR (400 MHz, $CDCl_3$): δ = 2.63 – 2.41 (m, 4H, $(CH_2)_2$-CF_2), 2.40 – 2.20 (m, 6H, P-CH_2), 1.70 – 1.41 (m, 12H, P-CH_2-($C\boldsymbol{H}_2$)$_2$), 0.98 (t, $^{3}J_{H/H}$ = 6.6 Hz, 9H, -CH_3).
$^{13}C\{^{1}H\}$ NMR (101 MHz, $CDCl_3$) δ = 119.99 (s, $N(CN)_2$), 23.93 (d, $^{3}J_{C/P}$ = 15.6 Hz, P-$(CH_2)_2$-($\boldsymbol{C}H_2$)), 23.56 (d, $^{2}J_{C/P}$ = 4.9 Hz, P-CH_2-$\boldsymbol{C}H_2$), 18.61 (d, J = 47.0 Hz, P-$\boldsymbol{C}H_2$), 13.30 (s, $\boldsymbol{C}H_3$).
$^{19}F\{^{1}H\}$ NMR (376 MHz, $CDCl_3$) δ = -80.93 (s, 3F, CF_3), -114.72 (s, 2F, CH_2-CF_2), -121.90 (s, 2F, CH_2-CF_2-$C\boldsymbol{F}_2$), -122.37 – -123.56 (m, 4F, CH_2-$(CF_2)_2$-($C\boldsymbol{F}_2$)$_2$), -126.23 (s, 2F, $C\boldsymbol{F}_2$-CF_3).
$^{31}P\{^{1}H\}$ NMR (162 MHz, $CDCl_3$): δ = 34.84 (s).

Figure S3.1: ^{1}H NMR spectrum of F6.

Figure S3.2: $^{13}C\{_1H\}$ NMR spectra of F6.

Figure S3.3: $^{19}F\{^1H\}$ NMR spectra of F6.

Figure S3.4: $^{31}P\{^{1}H\}$ NMR spectra of F6.

The most intense ESI –MS peaks were found to be: **ESI-MS(+Q)**: 549 Da. and **ESI-MS(-Q)**: 66 Da.

The experimental details of XPS characterization of the F6 ionic liquid are provided in the following paragraphs together with the XP-spectra and the curve fitting parameters.

S 4.1. Experimental - Small-area X-ray photoelectron spectroscopy (XPS)

A drop of ionic liquid F6 was deposited on a O_2-plasma cleaned silicon wafer which was then introduced into the spectrometer. The duration of exposure to air was less than three minutes. Before the deposition, the IL was stored in a vacuum chamber ($P \approx 10^{-5}$ mbar).

XPS analysis was performed using a PHI Quantera^{SXM} spectrometer (ULVAC-PHI, Chanhassen, MN, USA) equipped with an Al Kα monochromatic source (1486.6 eV). A beam diameter of 100 μm was employed. In standard mode, the photoelectrons were collected at an emission angle of 45°

and directed to the 32-channel detector system. The spectrometer is also equipped with a low-voltage argon-ion gun and a sample neutralizer for charge compensation. Calibration is regularly carried out using sputter-cleaned gold, silver, and copper as reference materials, according to ISO 15472:2009.

Survey spectra were acquired in fixed-analyser-transmission mode, selecting a pass energy of 280 eV, while the high-resolution spectra were collected with a pass energy of 69 eV.

Thanks to the external sample-positioning station, it was possible to select and record analysis areas at high magnification before placing the sample into the vacuum system. An electron-beam neutralizer was used to compensate for possible sample charging, and the spectra were further corrected referencing them to adventitious aliphatic carbon at 285.0 eV, when necessary (ASTM E 1523–03). The spectra were processed using CasaXPS (v2.3.19PR1.0, Casa Software Ltd., Wilmslow, Cheshire, UK).

S 4.2. XPS results: Ionic Liquid

A survey spectrum of the ionic liquid F6 shows the presence of the signals from the constituting elements: C, F, P, and N (Fig. S3). The C 1s, F 1s, P 2p, and N 1s narrow scan spectra were acquired. The detailed curve-fitting parameters are provided in Table S3 and the experimental quantitative analysis is consistent with the theoretical composition (Table S4).

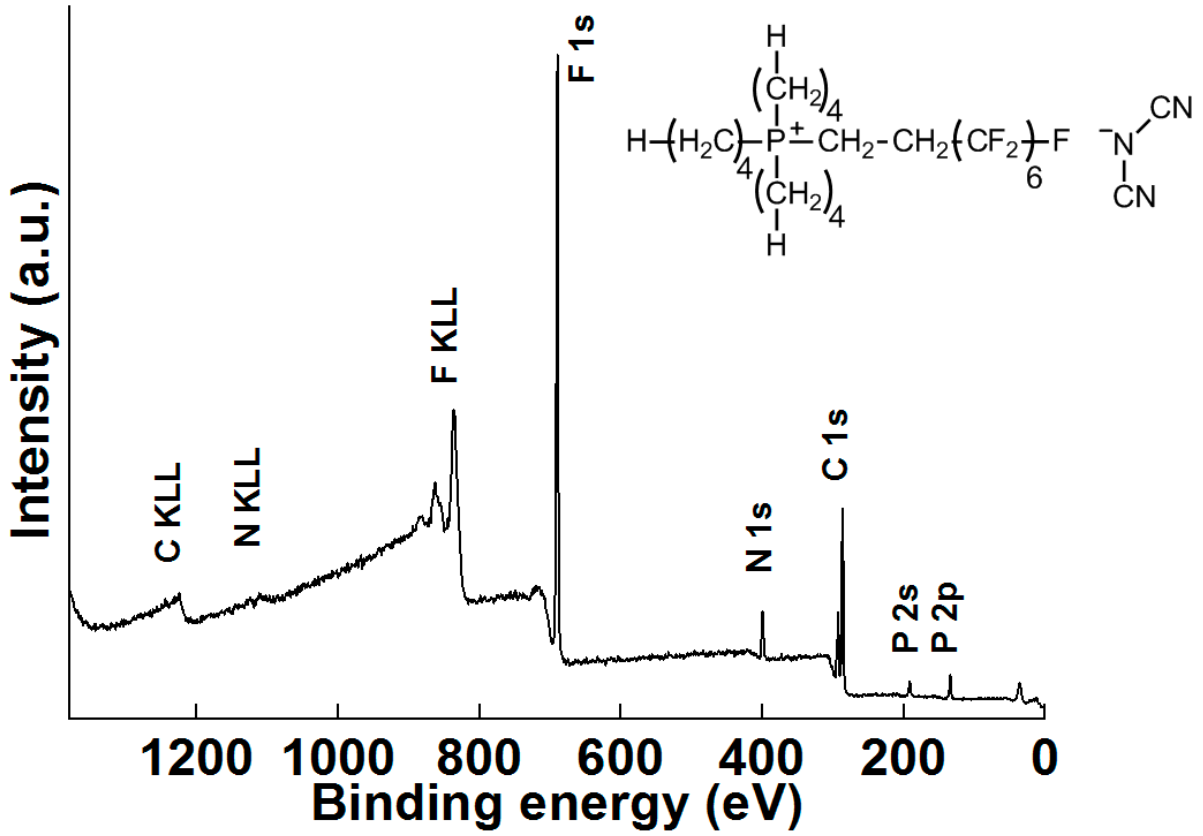

Figure S4. XPS survey spectra of the ionic liquid F6.

The C 1s signal is resolved by adapting six synthetic components to the experimental spectrum (Fig. S4 a). The peak at 285.0 eV is ascribed to aliphatic carbon[3] (area 41.16 %), the peak at 285.8 eV to the 4 methylene groups bounded to the phosphorus atom and to the methylene group prior to the perfluorochain of the cation[4] (22.64 %), and the peak at 286.7 eV to the two carbon atoms of the dicyanamide anion[3,5,6] (9.05 %). The three components at higher binding energy values are assigned to the carbons bounded to fluorine, particularly $\underline{C}F_2CH_2$ (291.0 eV, 4.52 %), CF_2 (291.9 eV, 18.10 %), and CF_3 (294.1 eV, 4.52 %)[3–6].

F 1s (Fig. S4 b) show the presence of a single component that is found at 689.2 eV for the F 1s signal attributed to the CF_x species[3–6].

The P 2p signal is fitted with a doublet due to the spin-orbit coupling. The P $2p_{3/2}$ peak is found at 132.7 eV[4,6], the P $2p_{1/2}$ peak is separated by 0.9 eV and their area ratio is 2:1 (Fig. S4 c).

The N 1s spectrum is composed of two components with a 2:1 intensity ratio (Fig. S4 d); the one at 398.1 eV is ascribed to nitrogen in the C≡N moiety[3,5] and the one at 399.4 eV is due to the $N_{C\text{-}N\text{-}C}$ atom[3,5].

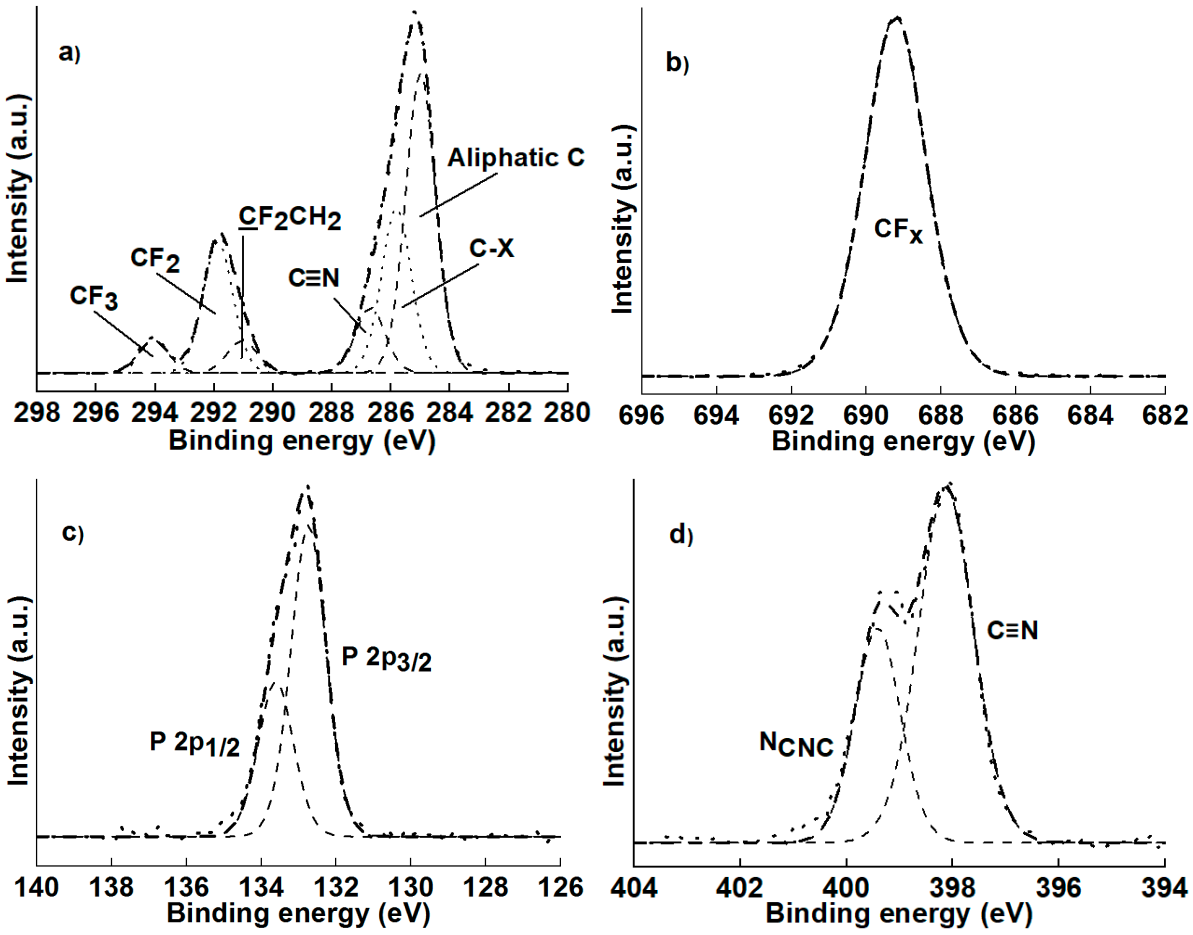

Figure S5. High-resolution XPS spectra of the ionic liquid F6. a) C 1s, b) F 1s, c) P 2p, d) N 1s.

Table S3. Curve-fitting parameters of C 1s, F 1s, P 2p, and N 1s signals of IL liquid

	Binding energy (eV)	Functional group	Line shape	FWHM (eV)
C 1s I	285.0(1)	Aliphatic C	GL(30)	1.2
C 1s II	285.8(1)	$\underline{C}H_2$-P, $\underline{C}H_2CF_2$	GL(30)	1.2
C 1s III	286.7(1)	C≡N	GL(30)	1.2
C 1s IV	291.0(1)	$CH_2\underline{C}F_2$	GL(30)	1.2
C 1s V	291.9(1)	CF_2	GL(30)	1.2
C 1s VI	294.1(1)	CF_3	GL(30)	1.2
F 1s	689.2(1)	CF_X	GL(40)	1.9
P $2p_{3/2}$	132.7(1)	Phosphonium	GL(30)	1.1
P $2p_{1/2}$	133.6(1)	Phosphonium	GL(30)	1.1
N 1s I	398.1(1)	C≡N	GL(30)	1.2
N 1s II	399.4(1)	$N_{C\text{-}N\text{-}C}$	GL(30)	1.0

Table S4. Quantitative composition (at%) of the ionic liquid F6 (accuracy 10%).

Element	**C**	**F**	**P**	**N**
Theoretical	56.4 at%	7.7 at%	2.6 at%	33.3 at%
Experimental	58.9 at %	6.6 at%	3.0 at%	31.5 at%

S 5. ICP-OES measurement of ionic liquid

The samples were weighed into 25 mL glass flasks and treated with 2 mL HNO_3 (conc.). After gentle heating (hot plate 100 °C) and cooling of the samples, the flasks were filled up to the calibration point with ultrapure water.

ICP-OES results for the ionic liquid F6 are listed in Table S5.

Table S5. ICP-OES analysis of the ionic liquid F6.

Element	**Ag**	**Ca**	**I**	**K**	**Na**
F6	26.0 ± 0.2 ppm	≤ 10 ppm	-	-	-

S 6. XPS Characterization of iron fluorides

The XPS narrow-scan spectra of Fe 2p and F 1s for iron(III) fluoride are shown in Figure S6.

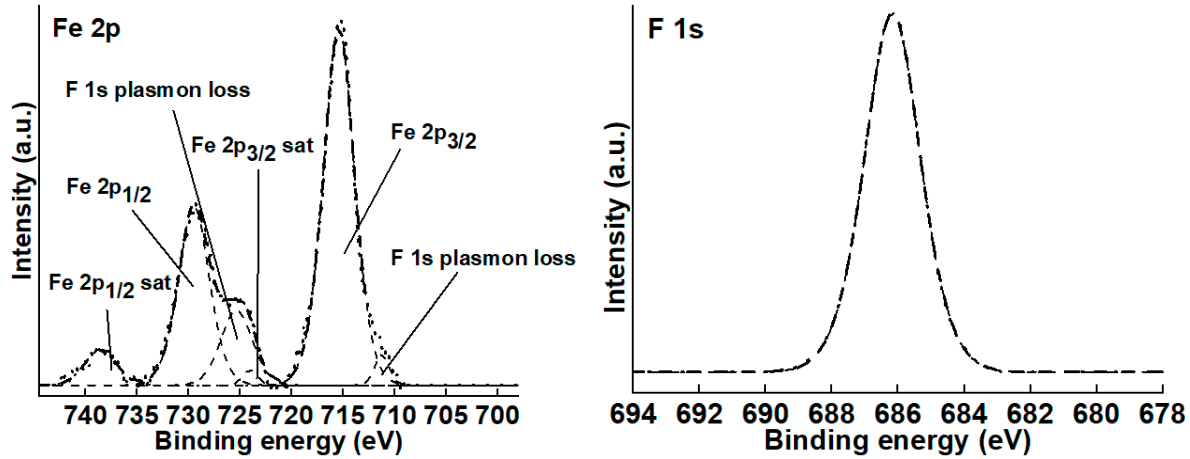

Figure S6. High-resolution XPS spectra acquired on FeF_3. Fe $2p_{3/2}$ = 715.4 eV. F 1s = 686.2 eV.

The XPS narrow-scan spectra of Fe 2p and F 1s for iron(II) fluoride are shown in Figure S7.

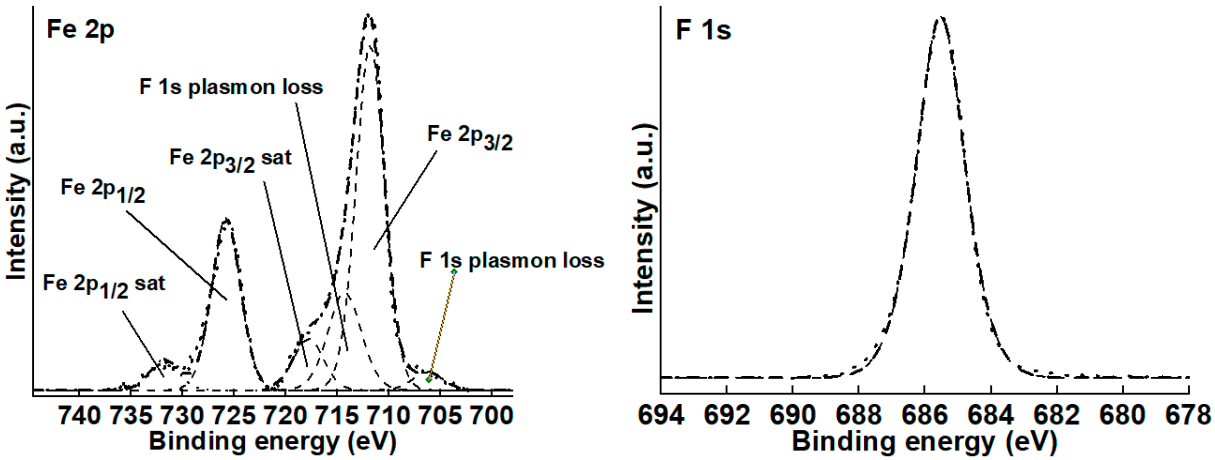

Figure S7. High-resolution XPS spectra acquired on FeF_2. Fe $2p_{3/2}$ = 711.6 eV. F 1s = 685.5 eV.

Attenuated Total Reflection Fourier Transform Infrared Spectroscopy

Experimental
Infrared spectra were acquired with an Alpha-P Bruker instrument equipped with a single-reflection-diamond-crystal ATR unit, in the range 4000-400 cm^{-1}, averaged over 64 scans.

The ATR FT-IR spectrum is provided in Figure S8.

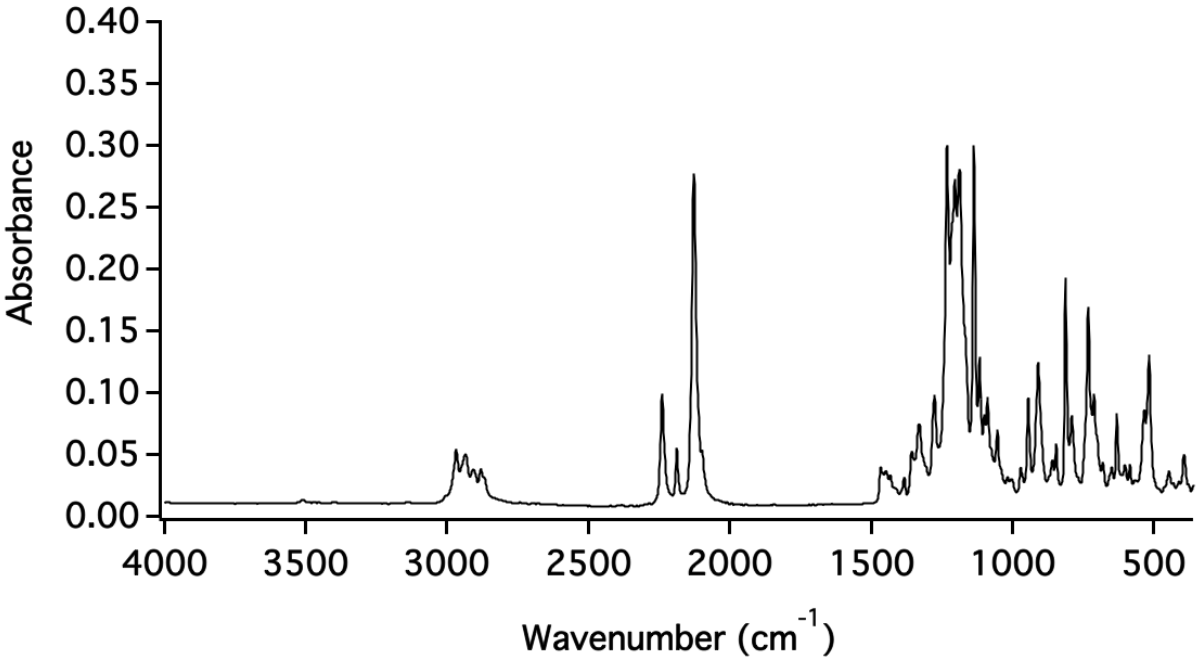

Figure S8. ATR FTIR spectrum of tributyl-3,3,4,4,5,5,6,6,7,7,8,8,8-tridecafluoro-octyl-phosphonium dicyanamide.

The ATR FTIR spectrum shows the following characteristic bands[7,8]: at 2900 – 3000 cm^{-1} the stretching vibrations from aliphatic C-H; between 2300 and 2000 cm^{-1} the signals attributable to the dicyanamide; and in the region 1400-1000 cm^{-1} the C-F stretching vibrations. At low wavenumbers, the vibrations that appear in the approximate range 650 – 750 cm^{-1} can be assigned to P-C (aliphatic bond).

A very small signal attributable to water can be detected at ca. 3550 cm^{-1}; this is better visible in the magnified region shown in Figure S9.

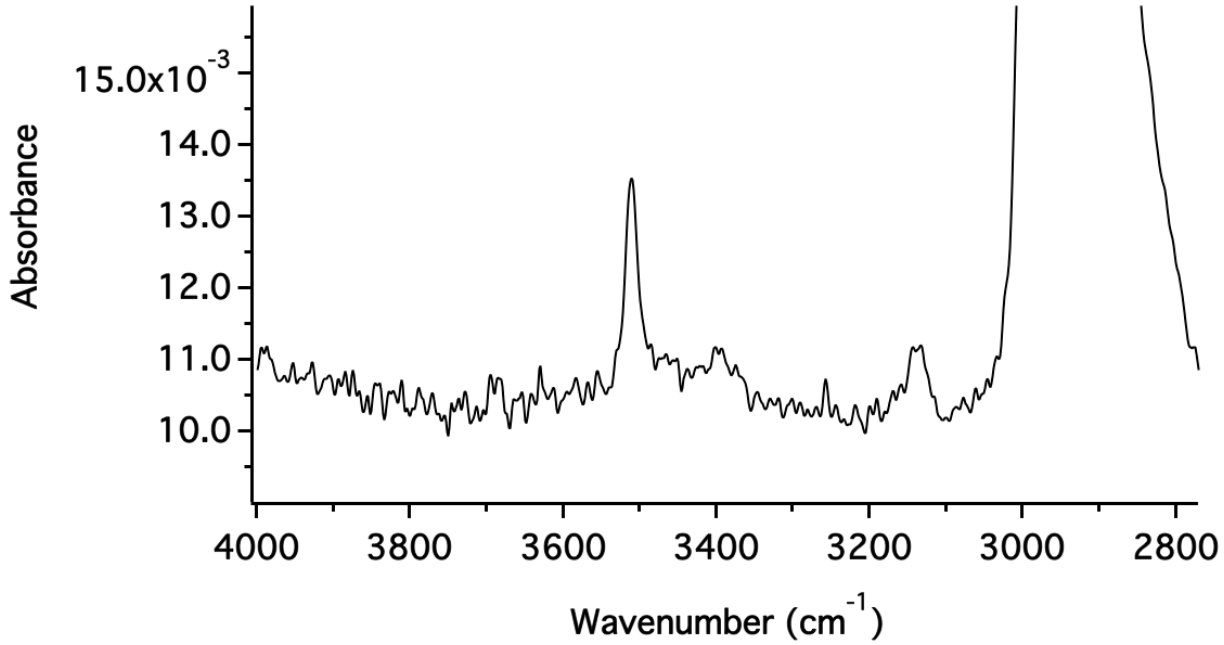

Figure S9. ATR FTIR spectrum of tributyl-3,3,4,4,5,5,6,6,7,7,8,8,8-tridecafluoro-octyl-phosphonium dicyanamide – magnification of the region around 3500 cm^{-1}.

S 7. Elastohydrodinamic (EHL) film-thickness formula

The sphere-on-plane geometry of the contact of the IL-lubricated steel counterparts was used to carry out the experiments presented in this work. In these conditions, it is possible to estimate the lubrication regime by using the Hamrock and Dowson formula[9]. The elastohydrodinamic (EHL) film thickness between the counterparts in relative motion was calculated by the formula reported in Figure S10. A legend is given in Table S6.

$$\frac{h_0}{R'} = 3.63\left(\frac{U\eta_0}{E'R'}\right)^{0.68}\left(\alpha E'\right)^{0.49}\left(\frac{W}{E'R'^2}\right)^{-0.073}\left(1 - e^{-0.68k}\right)$$

Figure S10. The elastohydrodynamic (EHL) film-thickness formula.

Table S6. Legend for the EHL film-thickness formula.

Simbol	Unit	Value	Meaning
h_0	m	1.25E-9	Minimum film thickness
R	m	0.002	Radius of curvature; 100Cr6 ball
R'	m	0.001	Reduced radius of curvature = R / 2 for ball-on-disk test
u	m/s	0.00125	Sliding speed
U	m/s	0.000625	Entraining surface velocity; in pure sliding, it is half sliding speed
η_0	Pa s	1.57	Viscosity at atmospheric pressure of the lubricant
E	Pa	2.1E+11	100Cr6 Young's modulus
v	adim	0.3	100Cr6 Poisson ratio
E'	Pa	2.31E+11	Reduced Young's modulus
α*	GPa^{-1}	10	Pressure-viscosity coefficient of the lubricant
W	N	5	Contact load
k	adim	1	Ellipticity parameter defined; k = 1 for spherical ball
Sq_A	m	9E-09	Roughness of the disk
Sq_B	m	1.40E-08	Roughness of the ball
RSM	m	1.7E-08	Composite roughness of the two contact surfaces = $(Rq_A^2 + Rq_B^2)^{\wedge}½$

* No data for the pressure-viscosity coefficient for F6 are available in the literature. We assumed a value of 10 GPa^{-1}, which is within the range measured by Pensado et al. for various fluorinated ILs.

An EHL film thick of ~ 3.2 nm is estimated for the tests carried out at 5 N and 1.25 mm/s.

The EHL film thickness was divided by the composite roughness of the tribopair (1.7 nm): a "λ ratio"[10,11] of 0.2 was found, suggesting that the sliding occurs in a boundary regime of lubrication[10-12]. On the other hand, due to the shear thinning behavior of the ionic liquid[13], the value is likely to be an overestimation.

S 8. XPS study of ionic liquid adsorption during 100Cr6 test

A mechanically polished 100Cr6 disk was stored in a vacuum chamber (P ≈ 10^{-5} mbar) overnight. A drop of the ionic liquid F6 was poured on the middle of the disk and the system was exposed to environmental air for 1 hour. The disk was then cleaned with ethanol and then introduced into the spectrometer. The aim of cleaning the 100Cr6 disk with ethanol was to remove the ionic liquid, in order to investigate how the IL/alloy system reacts if no tribostress is induced and when exposed to environmental air. Survey spectra and high-resolution spectra of the disk area before and after the contact with the ionic liquid were acquired. A beam diameter of 200 μm was used. Other details on XPS spectrometer are given in S 4.1.

S 8.1. Mechanically polished 100Cr6 disk

Survey spectra of the mechanically polished 100Cr6 disks revealed the presence of Fe, O, and C (Fig. S11). The Fe 2p, O 1s, and C 1s photoelectron signals were acquired as narrow-scan spectra.

The Fe $2p_{3/2}$ signal was resolved taking five components into account (Fig. S12 a): metallic iron at 706.9 eV[14,15], Fe(II) oxide and its satellites at 709.2 eV and 714.7 eV respectively[14-16], Fe(III) oxide at 710.6 eV[14,15], and Fe(III) oxy-hydroxide at 712.1 eV[14,15].

The O 1s spectrum shows the presence of four components (Fig. S12 b). The main peak (BE = 530.3 eV) [14,15] is attributed to iron oxide. The second peak at 531.6 eV is due to the presence of hydroxides[14,15]. The component for oxygen of carbonyl and carbonates is found at BE = 532.5 eV[14,15]. The fourth component at 533.7 eV is ascribed to the oxygen of adsorbed water[14].

The C 1s signal is composed of five components (Fig. S12 c). The peak at 283.2 eV is imputed to carbide[15,17]. All the other components are ascribed to the contaminants due to exposure to air: adventitious carbon: aliphatic carbon (BE = 285.0 eV)[18], C-O and C=O moieties (286.4 eV[18] and 287.8 eV[18,19]) and carboxyl and carbonates species (288.8 eV) [14,18,19].

Curve-fitting parameters are provided in Table S7.

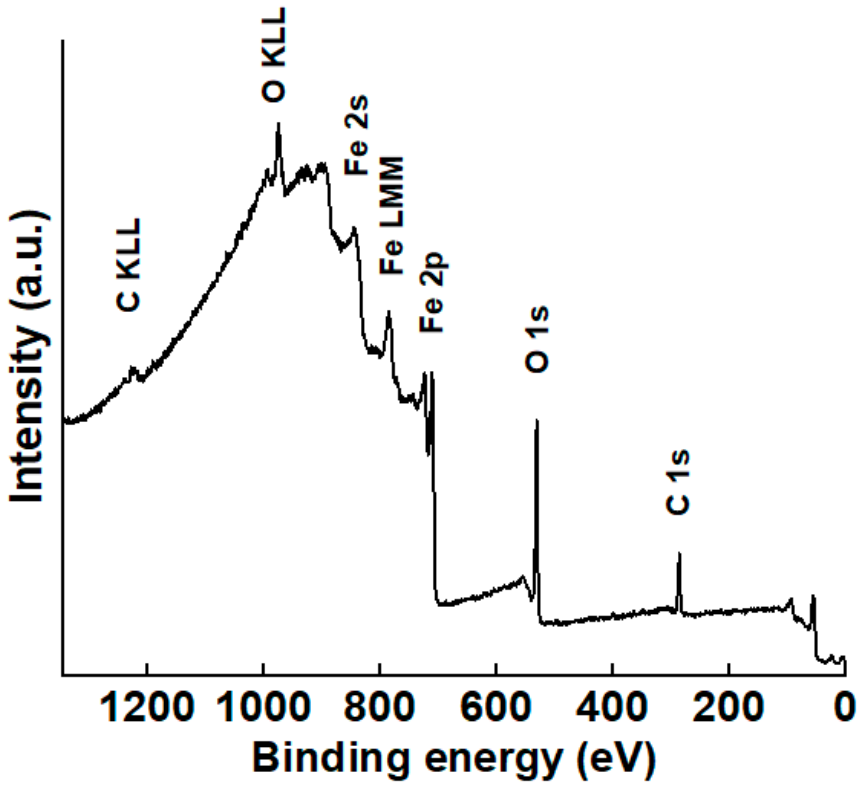

Figure S11. XPS survey spectra of the mechanically polished 100Cr6 disk. X-ray source: monochromatic Al Kα.

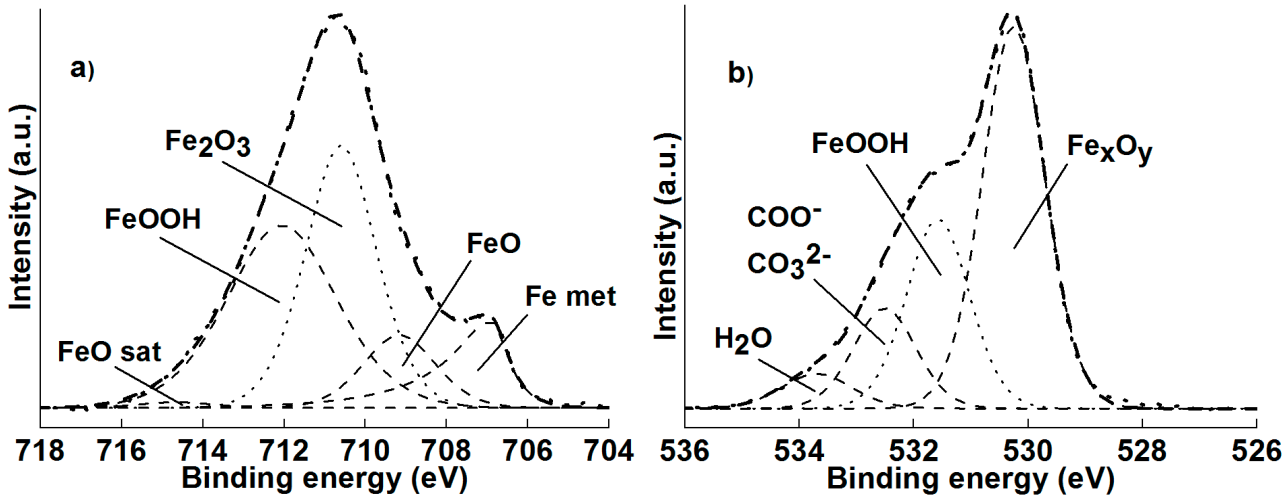

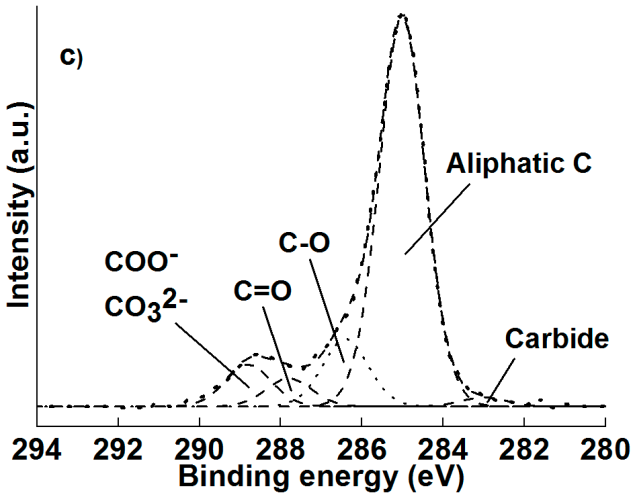

Figure S12. High-resolution XPS spectra of the mechanically polished 100Cr6 disk. a) Fe 2p, b) O 1s, c) C 1s.

Table S7. Curve-fitting parameters of Fe 2p, O 1s, and C 1s signals for the mechanically polished 100Cr6 disk.

	Binding energy (eV)	Functional group	Line shape	FWHM (eV)
Fe 2p I	706.9(2)	Fe(0)	GL(85)T(0.63)	1.0
Fe 2p II	709.2(1)	Fe(II)	GL(40)	2.1
Fe 2p III	714.7(1)	Fe(II) sat.	GL(40)	2.1
Fe 2p IV	710.6(1)	Fe(III)	GL(45)	2.0
Fe 2p V	712.1(1)	Fe(III) ox-hy	GL(45)	3.2
O 1s I	530.3(2)	Fe_XO_Y	GL(30)	1.3
O 1s II	531.6(2)	FeOOH	GL(30)	1.3
O 1s III	532.5(1)	COOX, carbonates	GL(30)	1.3
O 1s IV	533.7(1)	H_2O	GL(30)	1.5
C 1s I	283.0(1)	Carbide	GL(30)	1.3
C 1s II	285.0(1)	Aliphatic C	GL(30)	1.3
C 1s III	286.4(2)	C-O	GL(30)	1.3
C 1s IV	287.8(1)	C=O	GL(30)	1.3
C 1s V	288.8(1)	COOX, carbonates	GL(30)	1.3

S 8.2. 100Cr6 after ionic-liquid adsorption and cleaning

Wide scan spectra of the area where the ionic liquid was in contact with the 100Cr6 disk show the presence of Fe, O, P, C, Ca, F, and N (Fig. S13). High-resolution spectra of their most intense photoelectron signal were acquired (Fig. S14).

The Fe $2p_{3/2}$ signal showed the presence of five components (Fig. S14 a): metallic iron at 706.6 eV[14,15], Fe(II) oxide 709.3 eV with its satellites separated by 5.5 eV[14-16], Fe(III) oxide at 710.6 eV[14,15], and Fe(III) oxy-hydroxide at 712.1 eV[14,15].

The O 1s spectrum is resolved after curve fitting using four components (Fig. S14 b): iron oxides (BE = 529.9 eV) [14,15] and hydroxides (531.3 eV) [14,15], carbonyl and carbonates moieties (532.5 eV)[14,18,19], adsorbed water (533.8 eV)[14].

A doublet is fitted for the P 2p signal (Fig. S14 c). The P $2p_{3/2}$ peak is found at 132.7 eV and the P $2p_{1/2}$ peak at 133.6 eV (spin-orbit coupling energy separation 0.9 eV, area ratio 2:1). The signal is attributable to the phosphonium cation[4,6] (Table S1).

The C 1s signal is composed of nine components (Fig. S14 d). Together with the signals that might be due to the organic contamination layer at the surface of the alloy (aliphatic carbon 285.1 eV[18], C-O 286.6 eV[18], C=O 288.0 eV[18,19], carboxyl and carbonates species 288.9 eV[14,18,19]), one peak is attributed to the carbide (283.1 eV) [15,17] and some peaks might be related to the ionic liquid (C-P and C-F 285.9 eV, C≡N 286.6 eV, $\underline{C}F_2CH_2$ 291.2 eV, CF_2 292.2 eV, CF_3 294.2 eV)[3–6].

The Ca 2p signal is a doublet with the Ca $2p_{3/2}$ component at 347.6 eV and the Ca $2p_{1/2}$ separated by 3.6 eV at 350.9 eV (Fig. S14 e) and it might be ascribed to calcium fluoride[20] and calcium carbonate[21].

Two components fit the F 1s signal (Fig. S14 f). The most intense is due to the presence of CF_x moiety (689.2 eV)[1-5] and the second one might be associated to fluoride (684.3 eV) [20].

The N 1s spectrum shows two components (Fig. S14 g) that might be ascribable to the nitrogen of the IL anion; one peak is for the C≡N (398.5 eV)[1,3] and the other peak is for the $N_{N\text{-}C\text{-}N}$ atom (399.8 eV)[1,3].

Detailed curve fitting parameters are provided in Table S8.

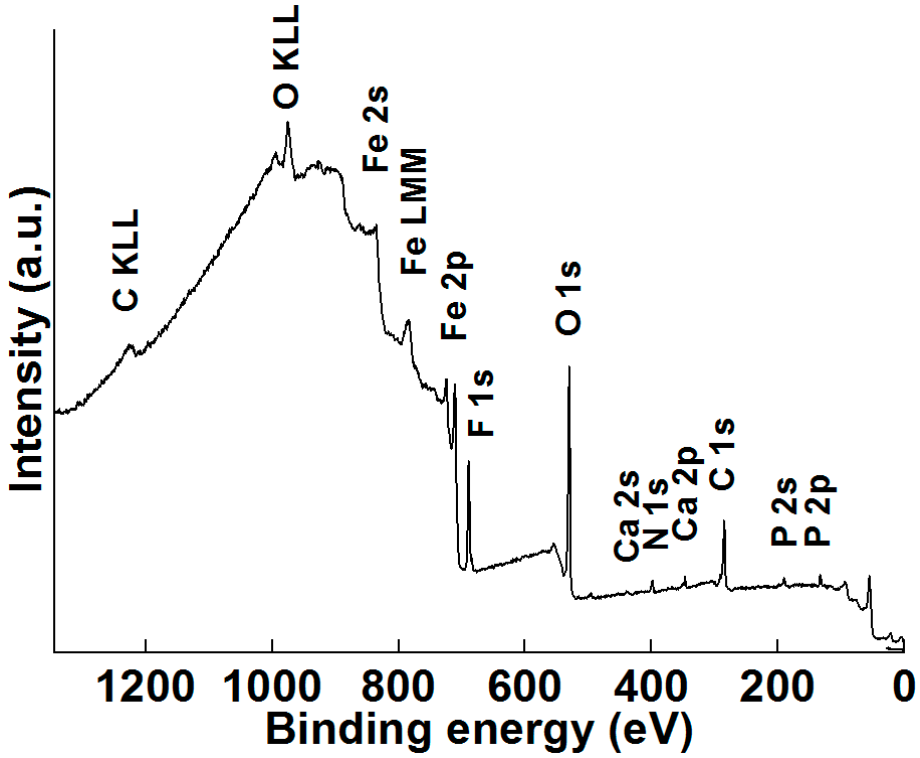

Figure S13. XPS survey spectra of the 100Cr6 disk area after adsorption of the ionic liquid F6 and cleaning.

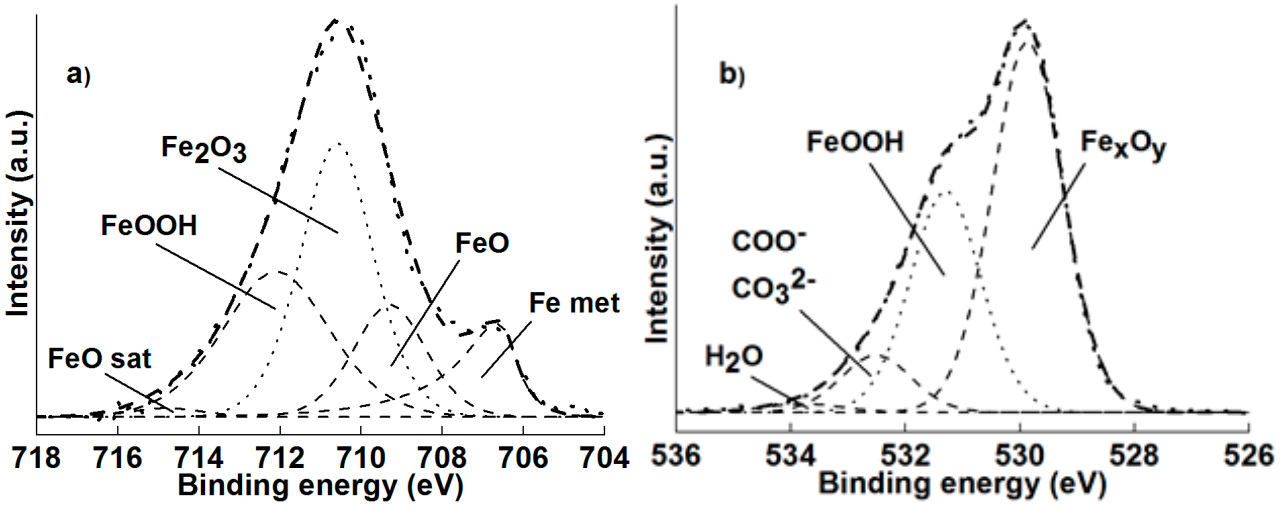

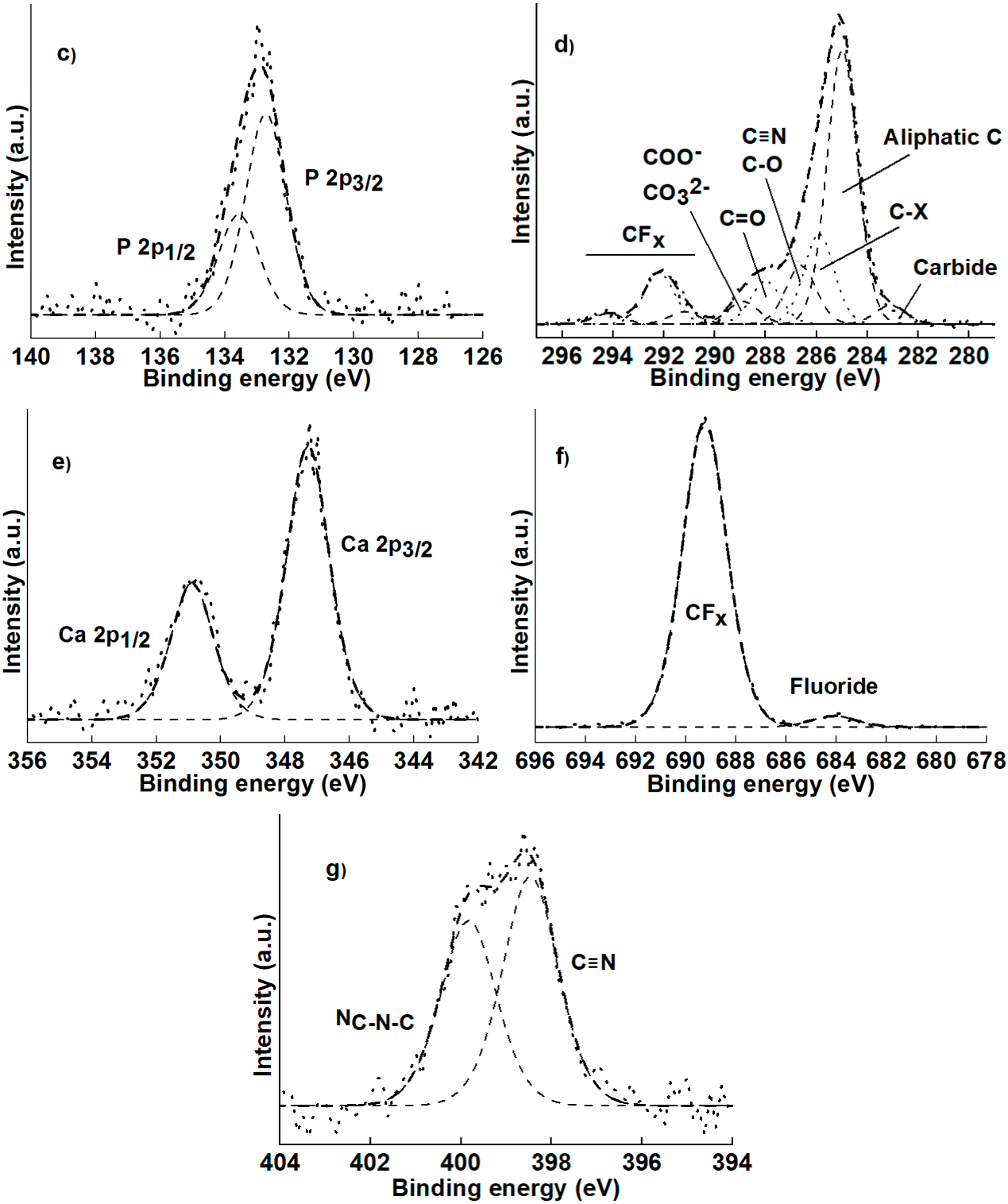

Figure S14. High-resolution XPS spectra of the 100Cr6 disk area after adsorption of the ionic liquid F6 and cleaning. a) Fe 2p, b) O 1s, c) P 2p, d) C 1s, e) Ca, f) F 1s, g) N 1s.

Table S8. Curve fitting parameters of Fe 2p, O 1s, P 2p, C 1s, Ca 2p, F 1s, and N 1s signals of the mechanically polished 100Cr6 disk after adsorption of ionic liquid F6 and cleaning.

	Binding energy (eV)	Functional group	Line shape	FWHM (eV)
Fe 2p I	706.6(2)	Fe(0)	GL(85)T(0.63)	1.0
Fe 2p II	709.3(1)	Fe(II)	GL(40)	2.1
Fe 2p III	714.8(1)	Fe(II) sat.	GL(40)	2.1
Fe 2p IV	710.6(1)	Fe(III)	GL(45)	2.0
Fe 2p V	712.1(1)	Fe(III) ox-hy	GL(45)	3.2
O 1s I	529.9(2)	Fe_XO_Y	GL(30)	1.4
O 1s II	531.3(2)	FeOOH, PO_4^{3-}	GL(30)	1.4
O 1s III	532.5(1)	COOX, carbonates	GL(30)	1.4
O 1s IV	533.8(1)	H_2O	GL(30)	1.6
P $2p_{3/2}$	132.7(1)	Phosphonium	GL(30)	1.5
P $2p_{3/2}$	133.6(1)	Phosphonium	GL(30)	1.5
C 1s I	283.1(1)	Carbide	GL(30)	1.4
C 1s II	285.0(1)	Aliphatic C	GL(30)	1.4
C 1s III	285.9(1)	$\underline{C}H_2$-P, $\underline{C}H_2CF_2$	GL(30)	1.4
C 1s IV	286.6(2)	C≡N, C-O	GL(30)	1.4
C 1s V	288.0(1)	C=O	GL(30)	1.4
C 1s VI	288.8(1)	COOX, carbonates	GL(30)	1.4
C 1s VII	291.2(1)	$CH_2\underline{C}F_2$	GL(30)	1.4
C 1s VIII	292.2(1)	CF_2	GL(30)	1.4
C 1s IX	294.2(1)	CF_3	GL(30)	1.4
Ca $2p_{3/2}$	347.6(1)	$CaCO_3$, CaF_2	GL(50)	1.5
Ca $2p_{1/2}$	350.9(1)	$CaCO_3$, CaF_2	GL(50)	1.5
F 1s I	684.3(1)	F^-	GL(40)	2.1
F 1s II	689.2(1)	CF_X	GL(40)	2.1
N 1s I	398.5(1)	C≡N	GL(45)	1.4
N 1s II	399.8(1)	$N_{C\text{-}N\text{-}C}$	GL(45)	1.4

References

[1]. Seah, M. P., Gilmore, I. S., Simplified equations for correction parameters for elastic scattering effects in AES and XPS for Q, β and attenuation lengths, *Surf. Interface Anal.* **2001**, 31, 835–846

[2]. Jablonski A., Database of correction parameters for the elastic scattering effects in XPS, *Surf. Interface Anal.* **1995**, 23, 29-37

[3]. Villar-Garcia, I. J., Smith, E. F., Taylor, A. W., Qiu, F., Lovelock, K. R. J., Jones, R. G., Licence, P., Charging of ionic liquid surfaces under X-ray irradiation: The measurement of absolute binding energies by XPS, *Phys. Chem. Chem. Phys*. **2011**, 13, 2797–2808

[4]. Blundell, R. K., Licence, P., Quaternary ammonium and phosphonium based ionic liquids: A comparison of common anions, *Phys. Chem. Chem. Phys*., **2014**, 16, 15278

[5]. Lovelock, K. R. J., Villar-Garcia, I. J., Maier, F., Steinruck, H.-P., Licence, P., Photoelectron spectroscopy of ionic liquid-based interfaces, *Chem. Rev.* **2010**, 110, 5158–5190

[6]. Niedermaier, I., Kolbeck, C., Taccardi, N., Schulz, P. S., Li J., Drewello, T., Wasserscheid, P., Steinruck, H.-P., Maier, F., Organic reactions in ionic liquids studied by in situ XPS, *Chem.Phys.Chem.* **2012**, 13, 1725 – 1735

[7]. Kiefera, J., Noack, K., Penna, T.C., Ribeiro, M.C.C., Weber, H., Kirchner, B., Vibrational signatures of anionic cyano groups in imidazolium ionic liquids, *Vibr. Spectroscopy*, **2017**, 91, 141 – 146

[8]. Daasch, L.W., Smith, D.C., Infrared Spectra of Phosphorus Compounds, *Anal. Chem.*, **1951**, 23, 853 – 868.

[9]. Hamrock, B. J., Dowson, D., Isothermal Elastohydrodynamic Lubrication of Point Contacts: Part III—Fully Flooded Results, *J. of Lubrication Tech.* **1977**, 99, 264-275

[10]. Tallian, T. E., On competing failure modes in rolling contact, *ASLE Trans.* 1967, 10, 428-439

[11]. Moyer, C. A., Bahney, L. L., Modifying the Lambda Ratio to Functional Line Contacts, *Trib. trans.* **1990**, 33, 535-542

[12]. book: Stachowiak, G., Batchelor, A. W., Engineering tribology, Butterworth-Heinemann: **2013**

[13]. Rauber, D., Zhang, P., Huch, V., Kraus, T., Hempelmann, R., Lamellar structures in fluorinated phosphonium ionic liquids: The roles of fluorination and chain length, *Phys. Chem. Chem. Phys.* **2017**, 19, 27251-27258

[14]. Elsener B., Pisu M., Fantauzzi M., Addari D., Rossi A., Electrochemical and XPS surface analytical study on the reactivity of Ni-free stainless steel in artificial saliva, *Mat. Corr.* **2016**, 67

[15]. Mangolini, F., Rossi, A. Spencer, N., Influence of metallic and oxidized iron/steel on the reactivity of triphenyl phosphorothionate in oil solution, *Tribo. Intern*., **2011**, 44, 670–683

[16]. Fantauzzi, M., Pacella, A., Atzei, D., Gianfagna, A., Andreozzi, G. B., Rossi, A., Combined use of X-ray photoelectron and Mössbauer spectroscopic techniques in the analytical characterization of iron oxidation state in amphibole asbestos, *Anal. Bioan. Chem.* **2010**, 396, 8, 2889-98

[17]. Wiltner, A., Linsmeier, Ch., Formation of endothermic carbides on iron and nickel, *Phys. Stat. Sol. A.* **2004**, 201, 881–887

[18]. Mangolini, F., Rossi, A., Spencer, N. D., Tribochemistry of triphenyl phosphorothionate (TPPT) by in situ attenuated total reflection (ATR/FT-IR) tribometry, *J. Phys. Chem. C* **2012**, 116, 5614–5627

[19]. Nedelcu, I., Piras, E., Rossi A., and Pasaribua, H. R., XPS analysis on the influence of water on the evolution of zinc dialkyldithiophosphate-derived reaction layer in lubricated rolling contacts, *Surf. Interface Anal*. **2012**, 44, 1219–1224

[20]. Nefedov, V. I., Salyn, Ya V., Leonhardt, G., Scheibe, R., A comparison of different spectrometers and charge corrections used in X-ray photoelectron spectroscopy, J. Electron Spectrosc. Relat. Phenom., **1977**, 10, 121-124

[21]. Stipp, S.L.S., Hochella, M.F. Jr, Structure and bonding environments at the calcite surface as observed with X-ray photoelectron spectroscopy (XPS) and low energy electron diffraction (LEED), *Geochim. Cosmochim. Acta*. **1991**, 55, 1723